Analytical Methods

Accepted Manuscript

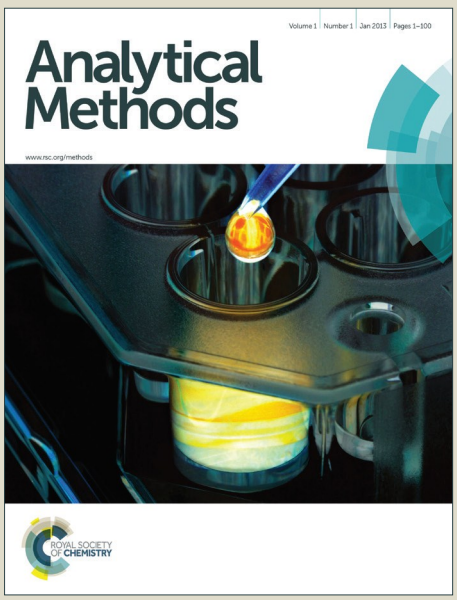

This is an *Accepted Manuscript*, which has been through the Royal Society of Chemistry peer review process and has been accepted for publication.

Accepted Manuscripts are published online shortly after acceptance, before technical editing, formatting and proof reading. Using this free service, authors can make their results available to the community, in citable form, before we publish the edited article. We will replace this *Accepted Manuscript* with the edited and formatted *Advance Article* as soon as it is available.

You can find more information about *Accepted Manuscripts* in the Information for Authors.

Please note that technical editing may introduce minor changes to the text and/or graphics, which may alter content. The journal's standard Terms & Conditions and the Ethical guidelines still apply. In no event shall the Royal Society of Chemistry be held responsible for any errors or omissions in this *Accepted Manuscript* or any consequences arising from the use of any information it contains.

ROYAL SOCIETY OF CHEMISTRY

www.rsc.org/methods

Journal Name

RSCPublishing

ARTICLE

Monitoring Dissolved Carbon Dioxide and Methane in Brine Environments at High Pressure using IR-ATR Spectroscopy

Thomas Schädle[a], Bobby Pejcic[b], Boris Mizaikoff[a†]

Cite this: DOI: 10.1039/x0xx00000x

Received ooth January 2012,
Accepted ooth January 2012

DOI: 10.1039/x0xx00000x

www.rsc.org/

Obtaining in situ information of greenhouse gases arising from deepwater environments is a challenge that has not been satisfactorily resolved to date. An infrared attenuated total reflection (IR-ATR) based on-line sensor system for detecting, monitoring, and differentiating carbon dioxide and methane in dissolved and gaseous states at different pressures (i.e., up to 6 MPa) in saline aquifer and/or synthetic brine environments is presented. It is demonstrated that the detection of dissolved CO_2 next to $^{13}CO_2$ and methane at pressurized conditions is possible at saline downhole conditions, and that gaseous vs. dissolved states of methane and CO_2 in aqueous environments may be differentiated using IR-ATR sensing techniques. Finally, it is shown for the first time that there are observable changes associated with distinctive infrared signatures of methane at the conditions of greenhouse gas storage mechanisms. This is of particular importance for advancing carbon capture and storage processes and fundamentally understanding the impact of emissions during the extraction of fossil-based fuels (i.e., shale, petroleum, etc.) from offshore environments.

Table of contents entry

An IR-ATR based on-line sensor system for monitoring greenhouse gases in brine environments is demonstrated. It is shown for the first time that there are evident changes of distinctive infrared signatures of methane and carbon dioxide at conditions relevant for greenhouse gas storage, which of particular relevance for understanding the subsurface behaviour of such gases after injection during carbon capture and storage (CCS) processes.

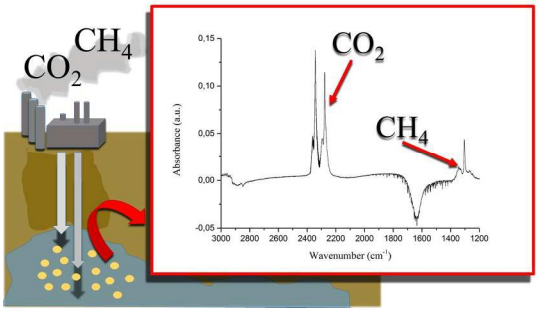

Introduction

In natural or artificial reservoirs, gases such as carbon dioxide or methane are usually in contact with aqueous environments.[1] The solubility of such gases in water is an important issue from an environmental perspective due to regulatory restrictions imposed on the hydrocarbon content in surface and ground waters. However, gas solubility data for most relevant reservoir gases as well as for volatile hydrocarbons at elevated pressure conditions and low temperatures ($T \leq 298.15K$) are scarcely reviewed to date. Consequently, the influence of such greenhouse gases and contaminants on ground water resources and aquifer systems is a topic of increasing global awareness.

The ocean plays an important role in exchanging and regulating gas levels in the biosphere. Recently, artificial reservoirs particularly in the tropics have been identified as significant contributors of CO_2 and CH_4 in the atmosphere[2-4]. The Petit Saut hydroelectric reservoir at the Sinnamary River in French Guiana is a typical example of a human-induced modification of the continental surface that has significantly changed the CO_2 and CH_4 exchange with the atmosphere[4]. Due to the microbial decomposition of flooded biomass primarily composed of tropical forest, this reservoir emits substantial amounts of CO_2 and CH_4 into the atmosphere[5]. Hence, various strategies including carbon capture and storage (CCS) aim at

preventing a more widespread dissemination of such gases. In order to decrease such human-induced contributions to atmospheric pollution, while at the same time potentially facilitating oil recovery, CCS or core flooding methods are investigated based on gas injection into saline reservoirs[6,7]. As these sequestration strategies aim at reducing greenhouse gas emissions by capturing and diverting them to a secure storage location, CO_2 is predominantly sequestered into geological formations via solubility trapping into the water phase of the otherwise solid formation [8].

These storage mechanisms lead to the inclusion of gaseous CO_2 trapped within the pore spaces, dissolution within the water phase, and long-term conversion of CO_2 into solid rock matrix[9]. Deep saline aquifers in sedimentary basins are potential sites for such sequestration strategies for CO_2. Such brine formations are the most common fluid reservoirs in the subsurface region prevalent around the world. Flow systems that involve water, CO_2, and dissolved ions have been extensively studied in geothermal reservoir engineering[10,11]. Hence, the development of robust on-line monitoring technologies facilitating advanced understanding on subsurface fluid and dissolution behaviour related to injected and stored gases in aqueous environments is demanded.

To date, various sensor technologies have been developed enabling monitoring of marine and downhole environments[12]. Concurrently, such sensing concepts are potentially equally suited as promising monitoring tools for gas dissolution monitoring scenarios. However, most sensor technologies reported to date are based on conventional laboratory equipment and analysis strategies rather than providing reliable devices suitable for in-field monitoring at the injection conditions of such gases into adequate storage compartments.

Mid-infrared (MIR) spectroscopy takes advantage of molecular vibration patterns at distinctive frequencies providing unique fingerprints of organic and inorganic molecules. Especially, infrared attenuated total reflection (IR-ATR) sensing techniques that are significantly less affected by interferences due to background absorptions of e.g., water appear ideally suited for studies in such aqueous environments, and have therefore recently emerged among the most promising in-field sensor technology for the detection of volatile organic constituents (VOCs) resulting from crude oil or refined product spillage[13] and chemical tracer molecules[14]. Moreover, spectroscopic techniques are particularly suited for investigating dynamic process, which enables additional insight on potentially relevant molecular interactions[15,16].

In the present study, we have developed an IR-ATR on-line sensor system for detecting and differentiating carbon dioxide in dissolved and gaseous states at different pressures (i.e., up to 6 MPa), which simultaneously facilitates methane detection. It is demonstrated that the quantitative detection of dissolved CO_2 next to $^{13}CO_2$ as well as dissolved methane at pressurized conditions is possible, and that gaseous vs. dissolved states of such gases in water may be differentiated. Using IR-ATR sensing techniques provides the basis for particularly robust, and highly miniaturizable sensing techniques that are readily adaptable for in-field applications at harsh environmental conditions. The geothermal studies performed to date mostly address higher temperatures and lower CO_2 pressures than would be encountered during aquifer disposal of sequestered CO_2. Consequently, the present work focuses on temperature and pressure ranges above and beyond these reported values, as they have not been covered by previous work to the best of our knowledge.

Instrumentation and Data Processing

A high pressure IR-ATR setup was realized combining the JetStream Circle Cell (Pike Technologies, Cottonwood, United States) with a Swagelok® connection to a gas-mixing/inlet system that is capable of handling 6 MPa of pressure. The pressure cell containing the ATR setup is made of stainless steel. A cylindrical ZnSe rod (approx. 82x6.4mm in dimensions) providing 12 internal reflections with an incident angle of 45° was used as the internal reflection element (IRE). The IRE is sealed with nitric butadiene rubber o-rings to the end caps of the pressure cell and is fully surrounded by the brine matrix.

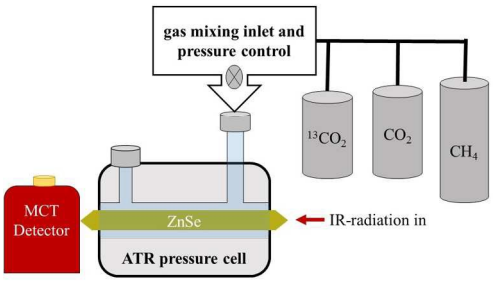

Figure 1. Schematic of the experimental setup including a high pressure IR-ATR system combined with a gas-mixing/inlet system.

The examined gases (CO_2, $^{13}CO_2$, CH_4) were directly injected into the sample chamber filled with the artificial saline solution (1.5mL sample volume) via the inlet valves of the gas mixing system. IR spectra were immediately recorded after opening the inlet valves in order to monitor the entire dissolution process of the gases, until equilibrium of the dissolution process was reached (i.e. no further changes in the IR signatures observable). Equilibrium conditions at elevated pressures were typically reached after a time period of 10 min. No further pumping system was needed to observe the dissolution process of these gases until equilibrium conditions.

IR-ATR spectra were recorded using a Bruker Vertex 70 FTIR spectrometer (Bruker Optics, Ettlingen, Germany) equipped with a liquid nitrogen cooled mercury-cadmium-telluride detector (MCT, Infrared Associates, Stuart/FL, United States). Spectral data were processed using the 'Essential FTIR' software package. Infrared absorption features were evaluated

via peak area analysis. For each measurement, 100 spectra were averaged at a spectral resolution of 0.5 cm^{-1}.

Results and Discussion

Monitoring of CO_2, $^{13}CO_2$, and CH_4 Dissolved in Synthetic Brine

To successfully monitor the behaviour of different gases in aqueous environments, it is anticipated that the respective IR absorption signatures are clearly discernible and spectrally sufficiently separated, thereby avoiding interferences among their individual gas absorption signatures and the background matrix. Figure 2 shows an example of the absorption signatures of CO_2, $^{13}CO_2$, and CH_4 in water after the dissolution process of these gases has reached equilibrium between gaseous and dissolved states. The spectra were recorded against the synthetic brine matrix as background at 4 MPa of pressure with all gas valves opened simultaneously.

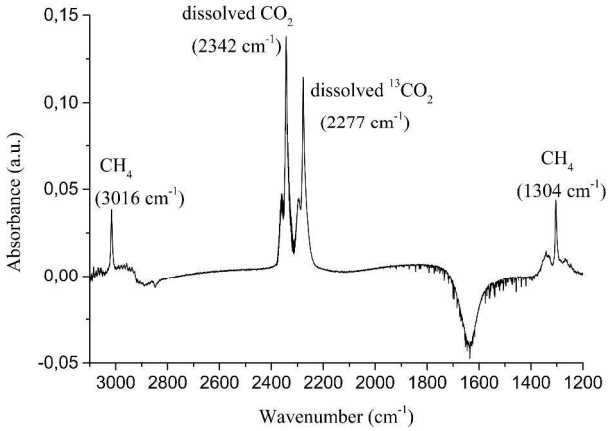

Figure 2. IR-ATR Spectra of dissolved greenhouse gases in aqueous environment (i.e., synthetic brine). The recorded spectrum shows the characteristic absorption features of CH_4 next to CO_2 and $^{13}CO_2$ dissolved in water recorded at 4 MPa of pressure and with 1 cm^{-1} spectral resolution, and an estimated concentration of 900 ppm (CH_4) and 5000 ppm (CO_2).

From the recorded IR spectra it is evident that the IR signatures of dissolved CO_2 at 2343 cm^{-1}, dissolved $^{13}CO_2$ at 2277 cm^{-1}, and methane at either 3016 cm^{-1} or 1304 cm^{-1} are clearly evident and sufficiently separated for enabling simultaneous detection and quantification of all three components side-by-side within the same sample solution. This is of particular importance for directly monitoring the behaviour and solution states of the different gases in saline water and downhole environments where carbon capture and storage is of interest and monitoring of several relevant constituents is required. The negative absorbance of the water band at 1620 cm^{-1} results from changes in the background spectrum due to injection of yet undissolved gases that were not present in the background spectra therefore causing negative absorbances by pushing water away from the IRE surface prior to dissolution. Water also usually shows a strong absorption feature at around 3000 cm^{-1}, which may lead to interferences with the methane 3016 cm^{-1} signature during long term monitoring of such dynamic processes. This is the reason why the methane 1304 cm^{-1} absorbance is used for further examination in this study.

Dissolved CO_2 and $^{13}CO_2$ in Saline Environments at Elevated Pressures

The typical absorption signature of gaseous CO_2 (2365 cm^{-1} and 2333 cm^{-1}) shifts to 2343 cm^{-1}, if CO_2 dissolves in water. Since the solubility of CO_2 in water is pressure dependent, more CO_2 will dissolve at higher pressures. At slightly increased pressures (i.e., up to approx. 0.6 MPa), the dissolution process from CO_2(g) to CO_2(aq) can actually be directly observed via the IR signatures of CO_2, as indicated by the arrows in Figure 3.

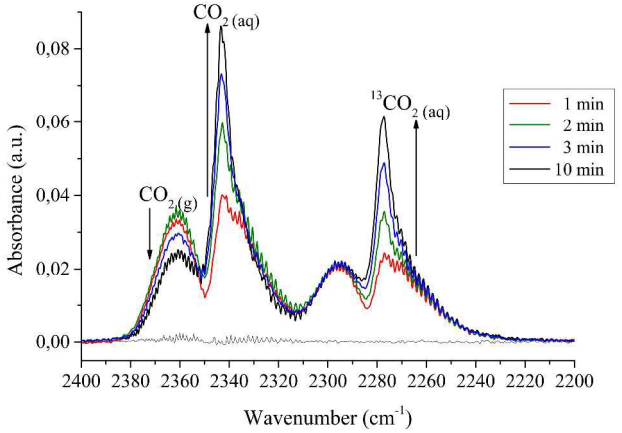

Figure 3. Dissolution of CO_2 and $^{13}CO_2$ in water over a period of 10 min. IR-ATR spectra were recorded at 0.5 cm^{-1} spectral resolution and at a pressure of 0.6 MPa.

Increasing the pressure from ambient conditions (0.1 MPa) to 0.6 MPa to dissolve more CO_2 in water results in a distinct increase of the absorption bands from CO_2(aq) at 2343 cm^{-1}, as evident in Figure 3. The light grey line represents the background absorption prior to the CO_2 injection into the IR-ATR sample cell. After 1 min (red line) of CO_2 injection at 0.6 MPa, both the CO_2(g) and CO_2(aq) signatures are already evident and clearly discernible. After 2 minutes (green line), a small increase in CO_2(g) is observable until all CO_2(g) according to the respective pressure value is evenly distributed within the sample chamber. Already after 3 minutes (green to blue line), the CO_2(g) signature decreases in intensity, whereas the intensity of the CO_2(aq) absorption band at 2343 cm^{-1} increases until saturation is reached (black line). After 10 minutes, no more changes in signal intensities could be observed leading to the assumption of equilibrium conditions within the sample cell.

Similar to dissolved CO_2 at 2343 cm^{-1}, its natural occurring isotope $^{13}CO_2$ shows a distinctive absorption feature, if dissolved in water. However, the absorption feature of dissolved $^{13}CO_2$ appears in the spectral range around 2277 cm^{-1}, thereby revealing a significant shift to lower wavenumbers of

65 cm^{-1} compared to the absorption signature of dissolved CO_2 located at 2343 cm^{-1}. This readily enables the direct evaluation – and discrimination - of dissolved $^{13}CO_2$ next to $^{12}CO_2$, which is particularly relevant for monitoring the behaviour of CO_2 at extreme conditions when injected together with $^{13}CO_2$ serving for example as a tracer molecule for carbon capture and storage processes[17]. The increase in absorption intensity with increasing pressure for $^{13}CO_2$ is shown in detail in Figure 4. The spectra represent the absorption signature of $^{13}CO_2$ after reaching equilibrium conditions (10-15 min) at the respective pressures.

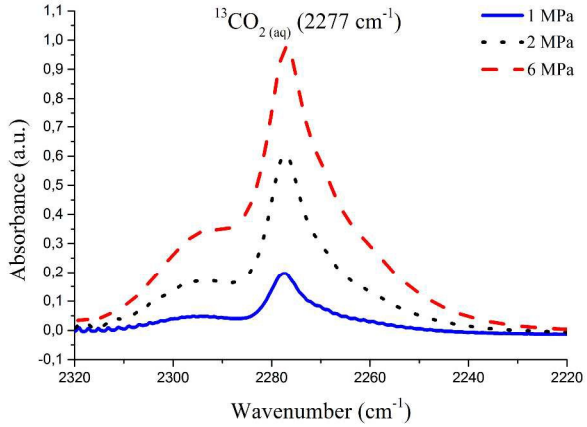

Figure 4. IR Spectra of $^{13}CO_2$ dissolved in water at different pressures. Dissolved $^{13}CO_2$ shows a distinctive absorption feature at 2277 cm^{-1}.

Methane Dissolved in Water at Elevated Pressures

The solubility of methane in water is a function of temperature and pressure. At ambient conditions, methane dissolves only slowly in water. Hence, by simply bubbling gaseous methane through water a less-than-measurable amount of methane (< 20 ppm at 20 °C) is dissolved at ambient conditions[18].

However, with temperatures approaching 0° C, higher salinity, and increasing pressure as present in deep sea environments, the solubility of methane is significantly increased[17]. Using the high pressure IR-ATR sensing system herein, methane in water was clearly detectable when increasing the pressure from 0.1 MPa (ambient conditions) to 0.4 MPa after manual baseline correction in the spectral region from 1320-1280 cm^{-1}. During the change of the pressure conditions, methane shows a minute shift to lower wavenumbers (approx. 2.5 cm^{-1}) of its absorbance maximum in the MIR, as shown in Figure 5. At low pressures (i.e., 0.4 MPa), the maximum of the methane absorption feature appears at 1305.5 cm^{-1}, with a second local maximum evident as a peak-shoulder at 1303 cm^{-1}. With increasing pressure, the absorption maximum is shifted to 1303 cm^{-1}. This shift may indicate the solution process of methane in water, as a shift of a vibrational absorption feature in the IR spectrum is usually related to a change of the force constant of the observed bond, which may be attributed to the formation of a hydration shell during the dissolution process

$$CH_4(g) \longrightarrow CH_4(aq)$$

However, the critical pressure for methane is 4.6 MPa, and close to this pressure regime the solubility of methane in water no longer follows a linear behavior[19], which reflects in the non-linear absorbance intensity changes evident in the spectra recorded > 4 MPa (orange and violet lines).

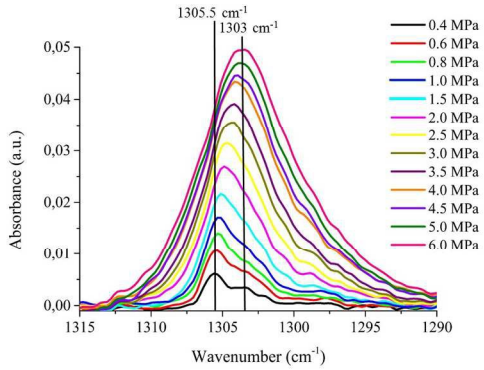

Figure 5. Wavenumber shift of the main methane absorption at increasing pressure conditions covering a concentration range of approx. 200-1000 ppm. The spectra were recorded by averaging 100 scans at a spectral resolution of 0.5 cm^{-1}.

For a more precise examination of this effect occurring during the dissolution process, an experiment was performed with the sample chamber of the IR-ATR system filled only with gaseous methane for comparing the IR signatures of gaseous and dissolved methane at similar conditions (i.e., 21°C, 4 MPa of pressure). The resulting IR spectra are illustrated in Figure 6.

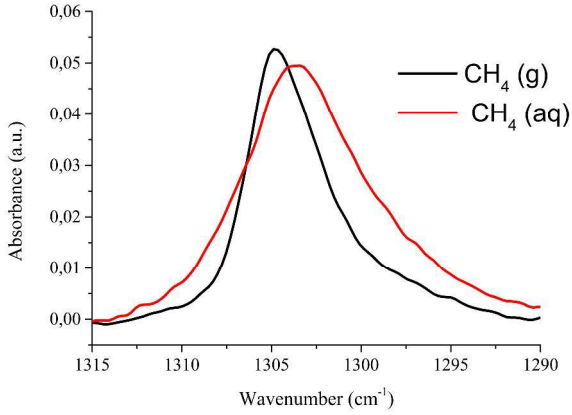

Figure 6. IR spectra of dissolved (red line) and gaseous (black line) CH_4 in water. The spectra were recorded at 4.5 MPa averaging 100 scans at a spectral resolution of 0.5 cm^{-1}.

The IR spectra of CH_4(g) (black line) and CH_4(aq) (red line) clearly reveal the difference in absorption maxima of methane in gaseous and dissolved state close to the critical pressure point. Gaseous methane shows no shift in peak intensity at pressures beneath the critical pressure, as compared to methane dissolved in a saline water matrix. Since the critical temperature

for methane is set at 190K, methane becomes supercritical beyond this limit and no discernible changes of the absorption features are evident. The IR signature of CH_4 in supercritical state is provided in Figure 7.

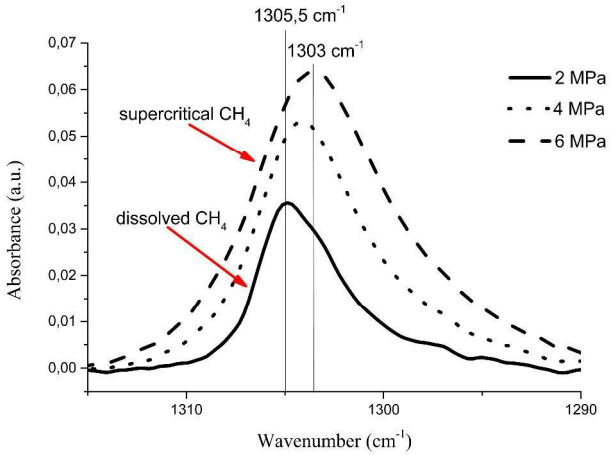

Figure 7. IR spectra of dissolved and supercritical CH_4 in brine. The spectra were recorded averaging 100 scans at a spectral resolution of 0.5 cm^{-1}.

Figure 7 clearly discriminates the different states of methane in aqueous environments via their IR signatures. The solid black line refers to dissolved CH_4, whereas the dashed lines refer to supercritical CH_4 in water with the absorption maximum at 1303 cm^{-1}. Hence, this shift in peak maximum enables the determination whether CH_4 may be stored in supercritical or dissolved state, if injected into saline reservoirs at high pressure conditions, which is of particular relevance for on-line monitoring purposes.

Multivariate Data Analysis and Sensor Calibration

Various models have been established for determining the dissolution processes of gases in aqueous environments. Most of these models are highly sophisticated and combine approximations of different theoretical models for simulating the physics that are involved in such complex gas-liquid systems. To date, there is no physical equation established that covers multi-component dissolution processes at high pressures, which renders quantitative calibrations for such scenarios an intricate task.

As a potential solution for data sets with a variety of potentially unknown changes during the measurements, multivariate data analysis strategies based on multicomponent regression methods appear suitable. Chemometric data evaluation approaches take advantage of statistical algorithms for maximizing the chemical information derived from e.g., multi-wavelength spectroscopic data recorded at highly variable and frequently unpredictable measurement conditions. Hence, in the present study multivariate regression models based on partial least squares (PLS) were established for deriving robust calibration models of the investigated multicomponent systems.

Four latent variables (LVs) were selected, which captured 99% of the variance within the calibration data set. Applying mean-centering and cross-validation as data preprocessing steps, the spectra used for calibration resulted in sufficiently robust quantitative calibration models. The influence of selected variables such as absorbance, related pressure and related wavelength within the calibration model may be evaluated using so-called selectivity ratios, i.e., the larger the value of the selectivity ratio, the more relevant the associated wavelength contributes to the prediction. Consequently, wavelengths with low selectivity ratios will be excluded for calculating the regression function for the calibrations. The selectivity ratios shown in Figure 8 correlate well with the investigated analytes, i.e., the highest values match up with the methane signature at 1305 cm^{-1} and the region of the carbon dioxide species from 2260- 2350 cm^{-1}. Hence, the PLS model weights the wavelengths of the gas absorbance signatures highest, which corresponds to the most relevant contributions within the spectral data sets.

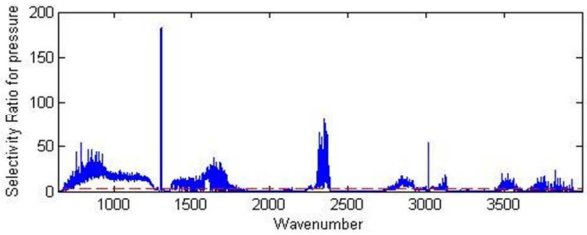

Figure 8. Selectivity ratio for establishing a multivariate regression model. The highest ratios match up with the relevant IR signatures of the dissolved molecules within the water matrix.

The calibration set used herein comprised three independent IR spectra recorded at four different pressures (0.6, 1.2, 2, and 4 MPa) covering the linear range of dissolution of the investigated gases. From these calibration samples, a linear regression model was established, as shown in Figure 9.

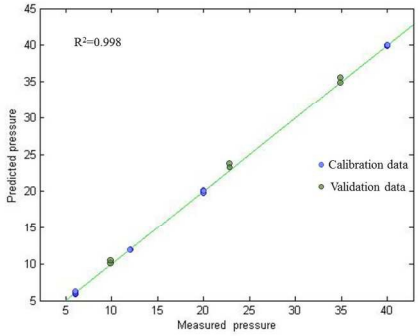

Figure 9. Calibration model for the investigated greenhouse gas mixtures in brine solution. The calibration data set included 3 independent spectra containing CO_2, $^{13}CO_2$, and CH_4 recorded at 4 different pressures resulting in a R^2=0.998.

The calibration model reveals a goodness-of-the-fit of R^2=0.998%, and suitably predicts the associated pressures. A set of spectra, which were recorded at different pressures (i.e., 1, 2.4, and 3.5 MPa), which were not included in the calibration

model were used as quasi unknowns for validating the established model. As anticipated, the predicted pressure values matched the actual pressure values very well, thereby confirming the robustness of the regression model. Figure 10 shows that the integrated peak areas of both the methane absorption band at 1305 cm^{-1} and the carbon dioxide absorption at 2343 cm^{-1}, which linearly correlates with both (i) the estimated concentration, and (ii) the ambient pressure at which the spectra were recorded. This correlation confirms that the direct evaluation of the methane and carbon dioxide absorption at relevant concentration levels reported in literature [17, 25-27] may be performed via direct peak area integration taking variable pressure conditions accurately into account. Although both signatures show a linear bahavior at the estimated concentrations, it is evident that methane is likely to appear at concentrations at least one order of magnitude lower than carbon dioxide in such mixtures, thus revealing significantly lower peak areas at the respective pressures.

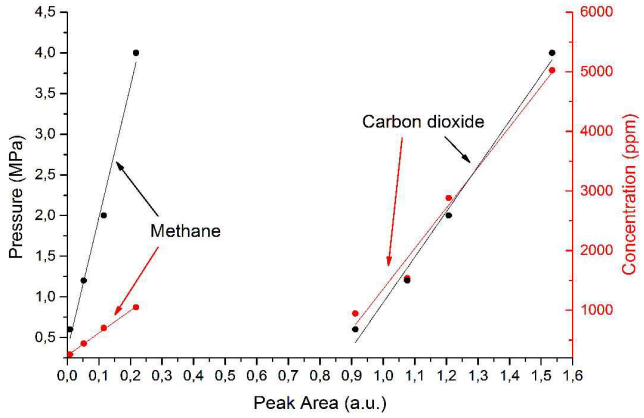

Figure 10. Integrated peak areas of the methane and carbon dioxide signatures. The red scale refers to the peak area against the estimated dissolved gas concentration[19,27] at different pressure values (black line), respectively.

Considering the linear relationship between pressure and peak area, the multivariate calibration model for predicting pressure conditions meets the desired requirements for monitoring such constituents at elevated pressure conditions in saline environments. Consequently, the predictions derived from the calibration model may be directly related to the linear behaviour of pressure vs. dissolvable amount of gas in these pressure ranges.

Experimental

Sample Processing

Carbon dioxide (99.5%) and methane (99.5%) were purchased from MTI IndustrieGase AG (Neu-Ulm, Germany). $^{13}CO_2$ (99.9%) was purchased from CAMPRO Scientific GmbH (Berlin, Germany). The JetStream Circle Cell IR-ATR accessory was purchased from Pike Technologies (Pike Technologies, Cottonwood, United States).

$MgSO_4$, Na_2SO_4, $CaCl_2$, KCl, and NaCl were purchased from VWR International GmbH, (Darmstadt, Germany). Deionized water was used as solvent for the salts to simulate saline environments[11].

The synthetic brine environment used as background matrix in this study was established by dissolving $MgSO_4$, Na_2SO_4, $CaCl_2$, KCl, and NaCl in deionized water following the composition given in Table 1.

Table 1. Composition of synthetic brine solution.

	g/L	wt-%
$MgSO_4$	12	4.9
Na_2SO_4	1.3	0.5
$CaCl_2$	14.8	6
KCl	0.7	0.3
NaCl	215	88.3

The compositions of saline aquifers around the world differ slightly in the concentration of dissolved salt, rock and/or sediment content. The composition used herein was adapted from Sell et al. (2013) for creating a representative brine environment.[11]

Conclusions

Using a synthetic brine solution as surrogate for real-world saline aquifer matrices, it was shown that IR-ATR spectroscopy is a useful analytical tool for on-line monitoring of changes in the gaseous, dissolved or supercritical states of greenhouse gases present in saline aquifers. This unique measurement concept ideally lends itself to applications in energy-related environmental monitoring scenarios aiming at capture and storage of such gases. To the best of our knowledge, the present study demonstrates for first time that changes of the characteristic methane IR signature in saline environments are detectable using IR-ATR spectroscopy at a wide range of relevant pressure conditions. Furthermore, a multivariate data evaluation strategy was developed establishing a robust calibration model for simultaneously quantifying CO_2, $^{13}CO_2$, and CH_4 in brine matrices. Taking advantage of thin-film IR waveguide technology[20-22] in combination with advanced infrared light sources such as quantum cascade lasers[22-24] promises robust, portable, and highly miniaturized IR analyzers deployable at harsh in-field conditions present in downhole and deep sea scenarios for monitoring of storage gases.

Acknowledgments

The authors greatly acknowledge the CSIRO Energy Flagship and the National Geosequestration Laboratory (NGL) for support of this study.

Notes and references

[a] Ulm University, Institute of Analytical and Bioanalytical Chemistry, Albert-Einstein-Allee1 11, 89081 Ulm, Germany.
[b] CSIRO, Energy Flagship, 26 Dick Perry Avenue, Kensington, WA 6151, Australia.
† Correspondence should be addressed to: boris.mizaikoff@uni-ulm.de

1 C. Galy-Lacaux, R. Delmas, G. Kouadio, S. Richard, P. Gosse, *Glob. Biogeochem. Cycles,* 1999, **13**, 503
2 C. Galy-Lacaux, R. Delmas, C. Jambert, JF. Dumestre, L. Labroue, S. Richard, *Glob. Biogeochem. Cycles,* 1997, **1,** 471
3 V. Saint Louis, C. Kelly, E. Duchemin, JWM. Rudd, DM Rosenberg, *BioScience*, 2000, **20**, 766
4 LP. Rosa, MA. Dos Santos, B. Matvienko, E. Sikar, R. Lourenco, CF. Menezes. *Hydrol. Process,* 2003, **17**, 1443
5 G. Abrila, S. Richard, F. Guerin, *Science of the Total Environment,* 2006, **354**, 246
6 S. Bachu, J.J. Adams, *Energy Convers. Manage.,*2003, **44**, 3151
7 P. Zhonghe, L. Yiman, F. Yang, D. Zhongfeng, *Applied Geochemistry*, 2012, **27**, 1821
8 O. Izgec, B. Demiral, B. Henri, S. Akin, *Transp Porous Med*, 2008, **72**, 24
9 R. Shiraki, T. Dunn, *Applied Geochemistry*, 2000, 15, 265
10 S. Schloemer, M. Furche, I. Dumke, J. Poggenburg, A. Bahr, C. Seeger, A. Vidal, E. Faber, *Applied Geochemistry,* 2013, **30**, 148
11 K. Sell, F. Enzmann, M. Kersten, E. Spangenberg, *Environ. Sci. Technol*. 2013, **47**, 198
12 R.D. Prien, *Marine Chemistry*, 2007, **107**, 422
13 T. Schädle, B. Pejcic , M. Myers, B. Mizaikoff, *Anal. Chem.,* 2014, **86**, 9512
14 F. Rauh, M. Schwenk, B. Pejcic, M. Myers, K.-B. Ho, L. Stalker, B. Mizaikoff, *Talanta*, 2014, **130**, 527
15 B.H. Stuart, "Infrared Spectroscopy: Fundamentals and Applications", Wiley, 2005, Hoboken, pp. 1 – 13
16 B. Mizaikoff, *Chem. Soc. Rev*., 2013, **42**, 8683
17 M. Myers, L. Stalker, B. Pejcic, A. Ross, *Applied Geochemistry, 2013,* **30**, 125
18 WF. Vogt, N. Pennington, B. Mizaikoff, Offshore Technology Conference Houston, Texas, U.S.A., 5–8 May 2003
19 D. Zhenhao, N Woller, J. Greenberg, J. Weare, *Geochimica and Cosmochimica Acta*, 1992, 56. 1451
20 C. Charlton, M. Giovanni, J. Faist, B. Mizaikoff, *Anal. Chem.* 2006, **78**, 4224
21 Lu, R.; Sheng, G.; Li, W.; Yu, H.; Raichlin, Y.; Katzir, A.; Mizaikoff, B.; *Angew. Chem. Int. Ed*. **2013**, 52, 2265 –2268
22 M. Sieger, F. Balluff, X. Wang, S.-S. Kim, L. Leidner, G. Gauglitz, B. Mizaikof , *Anal. Chem.* 2013, **85**, 3050
23 X. Wang, S.-S. Kim, R. Rossbach, M. Jetter, P. Michler, B. Mizaikoff, *Analyst* 2012, **137**, 2322
24 T. Schädle, A. Eifert, C. Kranz, Y. Raichlin, A. Katzir, B. Mizaikoff, *Appl. Spec*. 2013, **67**, 1057
25 C. Boulard, D.P. Connelly, M.C. Mowlem, *TrAC,* 2010, 29(2), 186.
26 S. Osborn, A. Vengosh, N. Warner, R. Jackson, *PNAS,* 2011, 108, 8172.
27 K. Pruess, N. Spycher*, Proceedings Tough Symp*., 2006. Berkeley, California.